IEEE Photonics Journal
An IEEE Photonics Society Publication

Open Access

Maskless Fabrication of Film-Patterned-Retarder (FPR) Using Wedged Liquid Crystal Cell

Volume 11, Number 6, December 2019

Doyeon Lee
Keumcheol Kwak
Chul Gyu Jhun
Hyun Seok Choi
Jang-kun Song

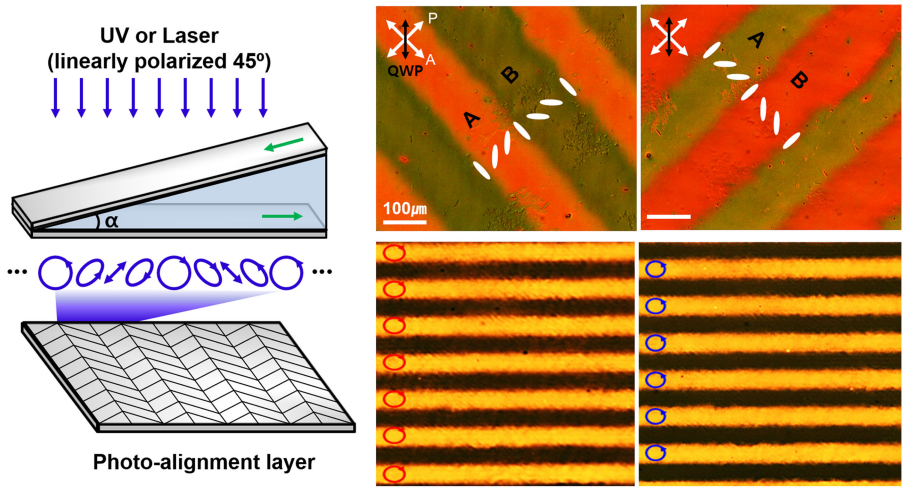

DOI: 10.1109/JPHOT.2019.2947402

IEEE photonics SOCIETY

IEEE

Maskless Fabrication of Film-Patterned-Retarder (FPR) Using Wedged Liquid Crystal Cell

Doyeon Lee,[1] Keumcheol Kwak,[1] Chul Gyu Jhun,[2] Hyun Seok Choi,[3] and Jang-kun Song [1]

[1]Department of Electrical and Computer Engineering, Sungkyunkwan University, Seoul 16419, South Korea
[2]Division of Electronic and Display Engineering, Hoseo University, Asan 31499, South Korea
[3]Samsung Advanced Institute of Technology, Samsung Electronics, Seoul 16678, South Korea

DOI:10.1109/JPHOT.2019.2947402

Manuscript received September 19, 2019; revised October 8, 2019; accepted October 10, 2019. Date of publication October 14, 2019; date of current version November 26, 2019.This work was supported by the National Research Foundation of Korea (NRF), funded by the Ministry of Science, ICT, and future planning under Grant NRF-2016R1A6A3A11934167. Corresponding author: Jang-Kun Song (e-mail: jk.song@skku.edu).

Abstract: Film-patterned-retarder (FPR) is an optical film used in the stereoscopic 3D display and is fabricated using an expensive photomask and nano-wire grid polarizer. This method is expensive and the pitch of FPR is fixed for a given photomask. Here, we introduce a maskless fabrication method for FPR using a wedged liquid crystal (LC) cell. The retardation of the wedged LC cell is continuously increased from one edge to the other. When the polarized monochromatic laser beam (450 nm) passes through the cell, periodically undulated polarization pattern of light is obtained, and can be used to produce FPR by combining with the photo-alignment method. The method does not require the expensive photomask and nano-wire grid polarizer, and the pitch of FPR can be simply controllable by changing the birefringence of LC material with temperature or using a light source of different wavelengths. Thus, this method can provide a simple and cost-effective method for FPR fabrication.

Index Terms: Stereoscopic display, wedge cell, polarization modulation, photo-alignment technique.

1. Introduction

The stereoscopic three-dimensional (3D) TV market had been rapidly growing from the late 2000s and it is collapsing owing to several reasons such as visual fatigue issue and lack of contents [1]. However, 3D display technology has found its niche markets in movie theaters, video games, and displays for medical instruments [2], [3]. Although holographic and volumetric technologies lead the state-of-art 3D technologies, the actual applications in the niche markets mostly use the glasses-type stereoscopic 3D technologies [4]–[10]. In theaters, two projectors with orthogonal polarization-directions project the two binocular images on a screen, and the cinema audiences wearing 3D glasses can see the binocular stereoscopic images separated into left and right eyes. Meanwhile, in the 3D displays for medical instruments such as visual acuity chart tester, a spatial division stereoscopic 3D display using a patterned birefringence film called film-patterned-retarder

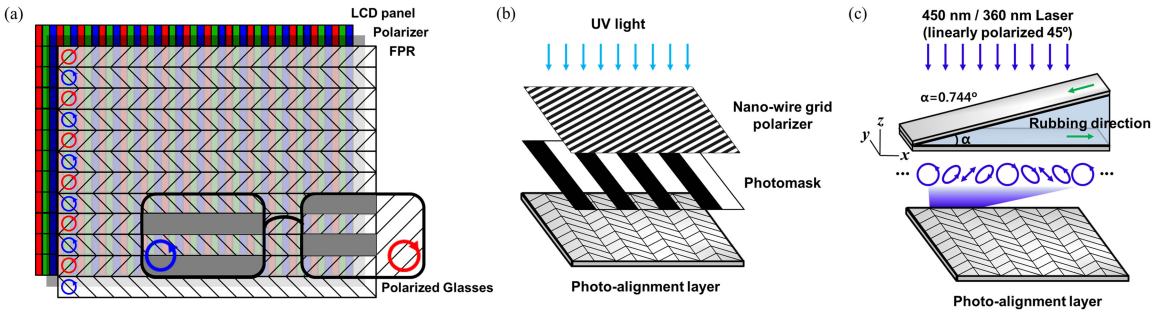

Fig. 1. (a) Principle of FPR using polarized glasses which have different circular polarization states on each side. (b) Conventional FPR fabrication method uses photomask and UV light. (c) Proposed FPR fabrication method uses wedge cell to create periodic phase retardation, photo-alignment layer, and monochromatic laser.

(FPR) is commonly used [11]. FPR makes two binocular images separated into two opposite circular polarization so that the watchers can see the stereoscopic images through 3D glasses. Thus, FPR is the key optical component to make the type of the stereoscopic 3D display function properly. In addition, a patterned phase retarder can be used to improve the viewing angle performance of a recent high-performance LCD with a wide color gamut using quantum dot [12].

To improve the performance of FPR, novel reactive-mesogen (RM) materials with reverse dispersion property has been developed so that the film can convert the light in the whole visible spectral range into circularly polarized light. In addition, the fabrication method based on photo-alignment of the RM layer has been also developed; cost-effective and roll-to-roll manufacturing processes are usually applied. This manufacturing process of FPR requisitely includes the photo-alignment step using an expensive photomask or zigzag nano-wire polarizer to fabricate a periodic pattern of retarders, in which the pitch of FPR is determined by the pitch of the photomask. FPR can be also fabricated by using nanoimprinting method, in which the liquid crystal (LC) alignment direction is determined by the imprinted surface morphologies [13], [14]. Although this method can have a high production yield and reliable pattern replication, the imprinting template needed in the process is highly difficult to fabricate and the pitch of FPR cannot be changed.

In this paper, we propose a novel and interesting approach to produce FPR without using a patterned photomask or zigzag nano-wired polarizer. The maskless FPR fabrication is achieved by using a wedged cell in which birefringence is continuously increased from one end to the other [15]–[18]. Linearly polarized light can be converted into periodically undulated polarization pattern from linear to circular polarization by the wedged LC cell, and that the optical axes switch orthogonally and periodically. Based on the principles, we demonstrate the fabrication method experimentally by combining the photo-alignment method using a laser beam, and we also explain the working mechanism theoretically. The proposed method provides a cost-effective and simple approach to fabricate FPR, and in addition, the pitch of FPR can be easily controlled.

2. Experimental Setup

Fig. 1(a) shows the structure of FPR and the working principle of 3D display using FPR. A 3D display is composed of a liquid crystal display (LCD) panel, a linear polarizer, and an FPR. The FPR converts the linearly polarized light from the LCD into two opposite circularly polarized light. When the image is observed through a circularly polarized glasses for 3D display, a stereoscopic image, that is, different images on two eyes are seen through the two opposite polarized glasses. Fig. 1(b) illustrates the conventional method using a nano-wire grid polarizer and stripe photomask. Usually, the exposures of ultraviolet (UV) light are performed twice on the photo-alignment layer; in the first exposure, the whole area is exposed to linearly polarized UV light without using a photomask, and then, the second shot of exposure is performed after inserting a stripe

photomask and rotating the polarization direction of linearly polarized UV light, which is orthogonal to the polarization direction of previous exposure. By the twice exposures of linearly polarized UV light, the zigzag patterned polarization direction is inlaid on the photo-alignment layer. Then, the RM layer is coated on the photo-alignment layer, and LC molecules in RM align along the zigzag pattern, producing the periodic stripe retarders, as illustrated in Fig. 1(b). Alternatively, a zigzag patterned nano-wire grid polarizer can be used instead of the linear nano-wire grid polarizer and the patterned photomask. In either case, the use of the expensive photomask or the zigzag nano-wire grid polarizer is essential to produce the periodic stripe pattern by the conventional method.

Fig. 1(c) illustrates the proposed new scheme for the maskless FPR fabrication. The method uses a wedged LC cell; the height of thicker side of the LC layer and the width of the wedge cell were approximately 0.5 mm and 38.5 mm, respectively, and the wedged angle, α, was around 0.744°. As a result, the thickness of the LC layer (d) gradually varies from 0 to 500 μm along x direction, since $d = x{\cdot}\tan\alpha$. The two glass substrates were coated with a commercial planar alignment layer used for in-plane switching technology (gifted by Samsung Display Company). The layers were treated by the anti-parallel rubbing process, and then, LC molecules align parallel to the wedge direction. The type of alignment layer used in the experiments produces pretilt angle below 1°, and we can neglect the influence of the pre-tilt angle on the effective phase retardation of our cell. The wedged cell was filled with one of typical LC mixtures, MLC-3003 and E7 (Merck Co., Korea). MLC-3003 has the birefringence (Δn) 0.125 at 450 nm and 0.155 at 360 nm, and E7 has 0.258 at 450 nm and 0.328 at 360 nm.

Linearly polarized diode-pumped solid-state (DPSS) lasers with the wavelength (λ) of 450 nm, 450M200 (Changchun Dragon Lasers Co., China), and 360 nm, MLL-FN-360 (CNI laser, China), were used as a light source in our experiment. Using a monochromatic laser beam allow us to neglect the influence of refractive index dispersion. That is, the polarization state of light after passing through the LC slap depends on the wavelength of light as well as the thickness of LC. Hence, when using a usual illumination having broad spectrum, the polarization state of light can be diverse depending on the wavelength. When the linearly polarized laser beam passes through the wedged LC cell at the polarization angle of 45° with respect to the rubbing direction in the LC cell, the polarization state of light is changed depending on the thickness of the wedge cell and birefringence of LC materials.

For the 450 nm laser source, we used an azo-dye layer as a photo-alignment layer. The azo-dye solution was prepared by adding 0.5 wt% of methyl red (MR) (Sigma-Aldrich) into 2-methoxyethanol (Sigma-Aldrich). The solution was sonicated for 30 minutes until MR was completely dissolved in the solvent. The azo-dye solution was spin-coated on a cleaned glass substrate at 2000 rpm for 60 seconds, and the substrate was cured on a hot plate at 70 °C for 10 minutes to evaporate the solvent. On the azo-dye coated substrate, the laser beam of 30 mW/cm^2 was exposed for 20 minutes through the wedged LC cell.

To examine the LC alignment on the azo-dye coated substrate, we fabricated an FPR cell using the azo-dye substrate and another substrate coated by the vertical alignment layer. The cell thickness was roughly 2 μm. In the cell, the azimuthal direction of LC alignment is governed by the alignment of azo-dye. An LC mixture, E7, was injected into the LC cell via capillary action, and the LC alignment state was observed using a polarized optical microscope (POM), BX53 (Olympus, Japan), in which a tungsten halogen lamp was used in the light source and the POM images appeared slightly yellowish.

For the 360 nm laser source, we used a commercial photo-alignment layer, ROP-103 (Rolic Co, Switzerland). The photo-alignment material was spin-coated on a cleaned glass substrate at 2000 rpm for 60 seconds, and the substrate was cured on a hot plate at 80 °C for 10 minutes. Then the layer was exposed by the 65 mW/cm^2 laser beam for 30 seconds through the wedged LC cell.

We fabricated FPR of the film type using the RMS03-013C (Merck Co., Korea). The RM material has the birefringence (Δn) 0.137, and the thickness was roughly 1 μm. On the exposed photo-alignment layer, we spin-coated the RM solution at 1000 rpm for 30 seconds, the substrate was cured on a hot plate at 60 °C for a 1 minute and then stayed at the room temperature for 1 minute.

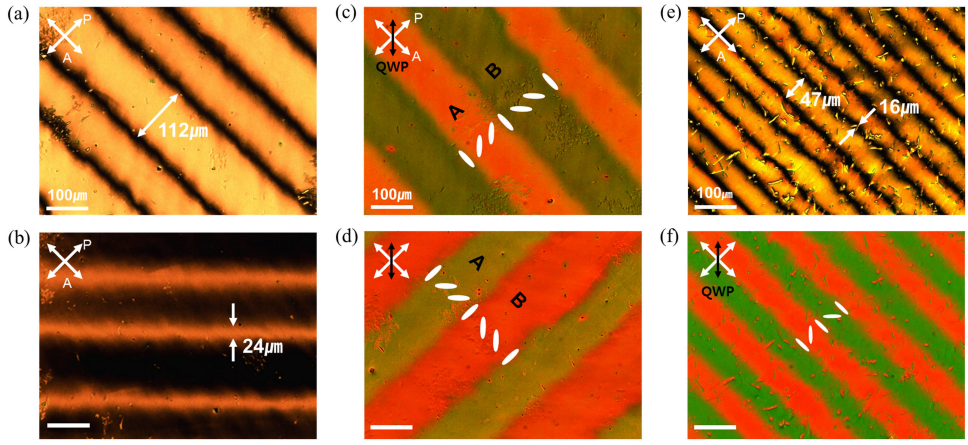

Fig. 2. (a)–(d) POM observation for the FPR using the wedged LC cells filled with MLC-3003 ($\Delta n = 0.125$), and (e, f) E7 ($\Delta n = 0.258$). (a), (b) The FPR cell has the pitch of 136 μm. When rotating the FPR cell by 45°, the brightness of wide domains and boundary lines are inverted. (c), (d) With QWP, the difference of A and B regions is highlighted. The alignment directions of LC molecules are indicated by the color of domains. (e), (f) The FPR cell with the E7 wedge cell has the same structure with the pitch of 63 μm.

Using the UV curing instrument, 2000-EC (DYMAX, USA), we photopolymerized the RM, and the FPR alignment state was analyzed using the POM.

3. Results

Fig. 2(a) and 2(b) show POM images under crossed polarizers for the FPR cell fabricated using the 450 nm laser source and the wedge cells injected with MLC-3003 (Δn = 0.125). The images clearly show the stripe domains with the pitch of approximately 136 μm separated by domain boundary lines. The bright domains have the width of about 112 μm and the boundary black lines is about 24 μm wide. In the top image with bright domains, the analyzer direction is parallel to the stripe. By rotating the FPR cell by 45°, the bright domains turned to dark and the dark boundary lines turned bright, indicating the 45° LC alignment in the domains with respect to the stripe direction, as shown in the bottom images. To clarify the LC alignment profile, we inserted a quarter wave plate (QWP) between the polarizer and analyzer, as shown in Fig. 2(c) and 2(d), where the black arrow indicates the optic axis of QWP. When the LC molecules are aligned parallel to the QWP axis, the total optical retardation increases, resulting in a red shift of the domain color. However, when the LCs are perpendicular to QWP, the domain becomes green owing to reduced retardation. Thus, the red and green colored stripes indicate the LC alignments in the neighboring domains are perpendicular to each other. By rotating the LC cell by 90°, the colors in the red and green domains are reversed, as shown in the bottom image of Fig. 2(c) and 2(d). Based on these POM observations, the LC molecular alignment profiles are analyzed as illustrated as the white ellipses in Fig. 2(c) and 2(d). The LCs are aligned having zigzag domains, and the LCs are parallel to the stripe in the boundary. Thus, these observations clearly show that the LC alignment in the FPR cell has the same optical structure as the usual FPR. If the polarization direction of the incident light is not 45° with respect to the rubbing direction of the wedged LC, the LC alignment directions in the two domains are not exactly orthogonal and the widths of the two domains can be slightly different, as shown in Fig. 2(a).

Fig. 2(e) and 2(f) shows the FPR cell fabricated using the wedge cell filled with E7 (Δn = 0.258), which has about twice higher birefringence than MLC-3003. The FPR cell exhibits the same stripe pattern with the periodic two-domain structure, but the pitch of the periodic pattern is about 63 μm, which is much shorter than that of Fig. 2(a). Thus, by changing the birefringence of LC material in

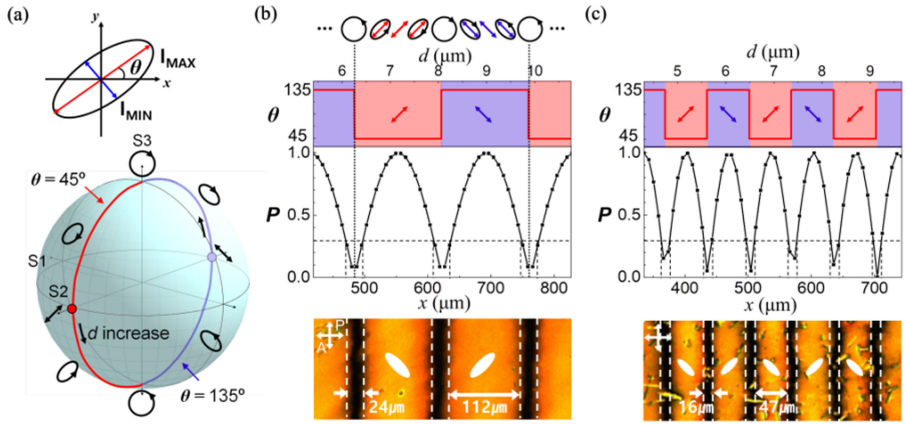

Fig. 3. (a) The polarization state of light after passing the wedged cell on the Poincaré sphere. The simulation results and experimental results for (b) $\Delta n = 0.125$ and (c) $\Delta n = 0.258$, respectively. The boundary lines in experimental results in (b) $\Delta n = 0.125$ and (c) $\Delta n = 0.258$ are well matched with the width in which the degree of polarization is less than 0.3.

the wedged cell, the pitch of the FPR can be simply changed. In this cell, excessive azo-dye was mistakenly added in the alignment layer. When excessive azo-dye is added in the alignment layer, the azo-dye can agglomerate to form a rod-like crystals during the spin-coating process, and the azo-dye crystal particles cause the defects in LC alignment, as shown in Fig. 2(e).

Even though the wedged LC cell does not have any periodic stripe pattern, the fabricated FPR exposed by laser beam through the wedged cell has the striped two-domain retarders under polarized microscope, whose optical axes are orthogonal each other. To figure out the underlying mechanism, we simulated the optical behavior in the system. When a linearly polarized light passes through an LC cell with the phase retardation ($=\Delta n d$), the phase difference ($\Delta\varphi$) between two optical axes of the cell is given by $2\pi\Delta n d/\lambda$, and the output polarization state can be determined using Jones vector as

$$\frac{1}{\sqrt{2}} E_0 \begin{pmatrix} 1 \\ \exp(i\Delta\varphi) \end{pmatrix} \tag{1}$$

As d increases, $\Delta\varphi$ between two basis axes in LC cell increases. Since d in the wedged LC cell gradually increases with respect to the position (x), the phase difference between two components in the Jones vector becomes a periodic function along x direction, which produces the periodic variation of polarization state. The polarization state can be geometrically expressed using the Poincaré sphere, as shown in Fig. 3(a). The circular locus on the Poincaré sphere is the polarization state of light after passing through the wedged cell as d increases. The curve circulates the Poincaré sphere along the longitudinal line periodically per every 2π increase of $\Delta\varphi$. Hence, the polarization state continuously changes from linear to circular polarization via elliptical polarization and vice versa periodically as d increases. Hence, the pitch of periodic polarization state variation after passing through the wedged cell can be expressed as $\lambda/(\Delta n \cdot \tan\alpha)$ along x direction.

When the polarized light with proper wavelengths is exposed on a photo-alignment layer, LC molecules are likely to align perpendicular to the polarization direction of light, that is, along the easy axis. As a result, the periodic variation polarization state of the light passing through the wedged cell is recorded on the photo-alignment layer. Since the two perpendicular LC domains appear within one cycle of polarization variation, the pitch of one domain is given as

$$p = \lambda/(2\Delta n \tan\alpha) \tag{2}$$

For the LCs having $\Delta n = 0.125$ and 0.258 in the 450 nm wavelength, the theoretical pitches are 138.6 μm and 67.2 μm, respectively, which well accord with the experimental results (136 μm and 63 μm, respectively).

Fig. 3(b) and 3(c) show the simulation results for the polarization state of the light passing through the wedged cell filled with MLC-3003 and E7, respectively. It is important to note that while the polarization state changes continuously, the long axis of the optical field, that is, the strongest electric field direction in each polarization state, switches abruptly between 45° and 135° when crossing the north and south poles on the Poincaré sphere. The red and purple arrows in the top illustration in Fig. 3(b) indicate the long axes of the optical field for each polarization state. The angle of the long axis of the optical field with respect to the horizontal axis (θ) is plotted in the upper part of the graphs in Fig. 3(b) and 3(c). In the red-colored region, the long axis of the polarization is along 45°, and the purple colored region has along 135°. The abrupt change of the long axis of the optical field explains how the FPR has two-perpendicular stripe domains with orthogonal retarders. Since the LCs align perpendicular to the long axis, the LCs within the red regions (45° optical axis) align along 135°, and the LCs within the purple regions align along 45°, producing the periodic FPR.

The lower parts of the plots in Fig. 3(b) and 3(c) represent the degree of linear polarization (P) defined by $(I_{MAX} - I_{MIN})/(I_{MAX} + I_{MIN})$, where I_{MAX} and I_{MIN} refer to the maximum and minimum intensities of the light transmitted through a linear polarizer when it is turned through the complete range of 360 degrees [19]. Here, the direction of I_{MAX} is the same with the long axis of the optical field. P periodically oscillates between 0 and 1. Note that here, the light with $P = 0$ does not mean the unpolarized light but mean that the intensity of light along two orthogonal axes are the same because of its circular polarization state. That is, the polarization states with the values of '0' and '1' correspond to circularly and linearly polarized light, respectively.

It is known that only a small difference of molecular population between the easy axis and its orthogonal axis can produce a uniform LC alignment along the easy axis in the photo-alignment technology. Hence, one does not need a perfectly polarized light to induce a uniform LC alignment on the photo-alignment layer. In our previous work, we investigated the relationship between the degree of polarization of exposed UV light on the photo-alignment layer and the alignment direction of LCs on the photo-alignment layer [20]. According to our previous work, when the degree of polarization is beyond 0.3, LCs align almost perfectly on the UV treated surface. In the POM images in Fig. 3(b) and 3(c), the thickness of boundary lines is rather thick; it is about 24 μm and 16 μm for the two FPR cells, respectively. The thickness of boundary lines matches well with the width in which the degree of polarization is less than 0.3, as illustrated in the plots in Fig. 3(b) and 3(c). For practical devices, these boundary lines should be minimized to improve the performance of FPRs. The presence of thick boundary lines can reduce the viewing angle margin. To reduce the width of the lines, a better photo-alignment material with higher sensitivity to polarized light is required.

In the next experiment, we used another photo-alignment layer, ROP-103 (Rolic Co, Switzerland), which is known as a high quality photoalignment material. Using ROP-103 and RMS03-013C, a FPR film was fabricated via the same wedged LC cell method. Fig. 4(a) shows the experimental setup for analyzing the fabricated FPRs. The FPR was inserted between a linear polarizer and an analyzer, where the analyzer is either of right or left circular polarizer. Fig. 4(b)–(d) and Fig. 4(e)–(g) are the POM images of the FPRs fabricated using the wedge cells injected with MLC-3003 ($\Delta n = 0.155$) and E7 ($\Delta n = 0.328$), respectively. The images in Fig. 4(b) and 4(e) were taken without inserting the analyzer. When linearly polarized light passes the FPR, the light in one group of domains turns into left circularly polarized light, and the light in the other domain groups turns into right circularly polarized light. Those in Fig. 4(c) and 4(f) were taken using a right circular polarizer (RCP) as an analyzer, and Fig. 4(d) and 4(g) were using a left circular polarizer (LCP) as an analyzer. We have optimized the film thickness to have a quarter wave plate for the middle range of visible light, i.e., between 550 and 650 nm. Given the Δn for the polymerized RM to be 0.137, we estimate the FPR film thickness to be approximately 1.05 ± 0.1 um. The clear dark stripe patterns under the RCP and LCP analyzers indicate that the stripe domains have almost perfectly the quarter

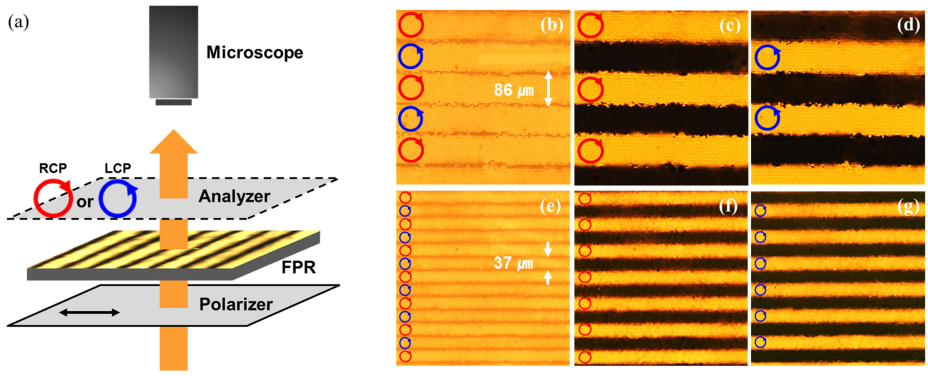

Fig. 4. (a) Experimental setup for analyzing the polarization states of FPR. (b)–(d) POM images of FPR using the wedged LC cells filled with MLC-3003 ($\Delta n = 0.155$), and (e)–(g) E7 ($\Delta n = 0.328$). (b) and (e) when the incident light is linearly polarized light and the analyzer is either (b), (e) removed or replaced with a circular polarizer, ((c), (f) RCP; (d), (g) LCP).

wave retardation with 90 degree rotation from each other in this range of wavelengths (550 to 650 nm), that is, the films show excellent properties as FPRs. In addition, the width of the boundary lines reduced to $\sim$9.5 μm, which is much thinner than those in the cells using azo-dye alignment layers. The result indicates that ROP-103 is a better photoalignment layer for our purpose. This provides sufficient performance for use in 3D displays. Broadband or achromatic performance can be achieved by further optimization of the LC mixture for the appropriate wavelength dispersion of the birefringence.

The periodic pitches of the FPRs in Fig. 4(b) and 4(e) are much different due to the birefringence difference between MLC-3003 and E7. The theoretical pitch can be obtained using Eq. (2). The theoretical pitches for the FPRs fabricated using the wedge cells filled with MLC-3003 and E7 were 89.4 μm and 42.3 μm, respectively. These are in good agreements with the experimental results (86 μm and 37 μm). These pitches are shorter than those obtained with the 450 nm laser exposure (138.6 μm and 67.2 μm, respectively).

4. Conclusions

We proposed the maskless fabrication method for FPR using a wedged LC cell and a monochromatic laser beam, without a photomask or patterned nano-wire grid polarizer. The proposed method is cost–efficient. Moreover, the method provides a wide flexibility for controlling the pitch of the FPR via changing the light source wavelength, wedge cell angle, as well as the composition and the working temperature of the LC mixture. We demonstrated the feasibility of the method and explained the working mechanism theoretically. The periodic variation of polarization state of light passing through a wedged cell is used to induce the periodic LC alignment. In particular, the binary change of the long axis of the optical field in the periodic polarization state is the key factor to induce the two domain retarders. Further improvements of the method should target the width of the boundaries between the domains. This will improve the stray light of the devices manufactured by this method. This can be achieved either by increasing the degree of linear polarization in the vicinity of the domain boundaries or by finding a good photo-alignment layer working in a lower degree of polarization. The ROP-103 has demonstrated the advantage over an azo-dye type photo-alignment layer, but further research may be required. The FPR produced by this method can be utilized for lower cost manufacturing of stereoscopic 3D displays.

References

[1] L. Zhang, Y. Q. Zhang, J. S. Zhang, L. Xu, and J. B. Jonas, "Visual fatigue and discomfort after stereoscopic display viewing," *Acta Ophthalmologica*, vol. 91, pp. e149–e153, 2013.

[2] J. P. McIntire, P. R. Havig, and E. E. Geiselman, "Stereoscopic 3D displays and human performance: A comprehensive review," *Displays*, vol. 35, pp. 18–26, 2014.

[3] R. T. Held and T. T. Hui, "A guide to stereoscopic 3D displays in medicine," *Academic Radiol.*, vol. 18, pp. 1035–1048, 2011.

[4] Y. J. Wu, Y. S. Jeng, P. C. Yeh, C. J. Hu, and W. M. Huang, "Stereoscopic 3D display using patterned retarder," in *Proc. SID Symp. Dig. Tech. Papers*, 2008, pp. 260–263.

[5] T. Inoue and H. Ohzu, "Accommodative responses to stereoscopic three-dimensional display," *Appl. Opt.*, vol. 36, no. 19, pp. 4509–4515, 1997.

[6] M. A. Wenzel *et al.*, "EEG-based usability assessment of 3D shutter glasses," *J. Neural Eng.*, vol. 13, 2016, Art. no. 016003.

[7] S. M. Jung *et al.*, "25.4 L: Late-news paper: A novel polarizer glasses-type 3D displays with an active retarder," in *Proc. SID Symp. Dig. Tech. Papers*, 2009, pp. 348–351.

[8] Y. J. Lim *et al.*, "Film patterned retarder for stereoscopic three-dimensional display using ink-jet printing method," *Opt. Exp.*, vol. 22, no. 19, pp. 22661–22666, 2014.

[9] J. H. Lee *et al.*, "Novel film patterned retarder utilizing in-plane electric field," *Opt. Exp.*, vol. 22, no. 12, pp. 15315–15319, 2014.

[10] M. S. Park, S. Y. Kim, and S. Y. Ryu, "Macroscopic alignment control of liquid crystal molecule in optical film for 3D display," *Mol. Cryst. Liquid Cryst.*, vol. 605, pp. 275–280, 2014.

[11] R. Smith, A. Day, T. Rockall, K. Ballard, M. Bailey, and I. Jourdan, "Advanced stereoscopic projection technology significantly improves novice performance of minimally invasive surgical skills," *Surgical Endoscopy*, vol. 26, pp. 1522–1527, 2012.

[12] H.-W. Chen, J.-H. Lee, B.-Y. Lin, S. Chen, and S.-T. Wu, "Liquid crystal display and organic light-emitting diode display: Present status and future perspectives," *Light, Sci. Appl.*, vol. 7, 2018, Art. no. 17168.

[13] Z. He, Y.-H. Lee, R. Chen, D. Chanda, and S.-T. Wu, "Switchable Pancharatnam–Berry microlens array with nano-imprinted liquid crystal alignment," *Opt. Lett.*, vol. 43, pp. 5062–5065, 2018.

[14] Z. He, G. Tan, D. Chanda, and S.-T. Wu, "Novel liquid crystal photonic devices enabled by two-photon polymerization," *Opt. Exp.*, vol. 27, pp. 11472–11491, 2019.

[15] R. Laberdesque, A. Jullien, U. Bortolozzo, N. Forget, and S. Residori, "Tunable angular shearing interferometer based on wedged liquid crystal cells," *Appl. Opt.*, vol. 56, pp. 8656–8662, 2017.

[16] J. Kedzierski, Z. Raszewski, M. Kojdecki, J. Zielinski, E. Miszczyk, and L. Lipinska, "Optical method for determining anisotropy of diamagnetic susceptibility of nematic and polar anchoring energy coefficient of nematic-substrate systems by using a cell of varying thickness," *Optoelectron. Rev.*, vol. 12, pp. 299–304, 2004.

[17] K. Kowiorski *et al.*, "Application of modified interference wedge method in measurements of indices of refraction and birefringence of nematic liquid crystals," *Acta Physica Polonica A*, vol. 124, pp. 946–948, 2013.

[18] D. Chen *et al.*, "Interference-free and single exposure to generate continuous cycloidal alignment for large-area liquid crystal devices," *Opt. Exp.*, vol. 27, pp. 29332–29339, 2019.

[19] S. Trippe, "Polarization and polarimetry: A review," 2014, *arXiv:1401.1911.*

[20] J.-K. Lim and J.-K. Song, "Polymerized micro-patterned optical birefringence film and its fabrication using multi beam mixing," *Opt. Exp.*, vol. 19, no. 27, pp. 26956–26961, 2011.